Published online 23 July 2011 *Nucleic Acids Research, 2011, Vol. 39, No. 20* ***8901–8914***
doi:10.1093/nar/gkr605

hnRNP Q mediates a phase-dependent translation-coupled mRNA decay of mouse *Period3*

Do-Yeon Kim[1], Eunyee Kwak[1], Sung-Hoon Kim[2], Kyung-Ha Lee[1], Kyung-Chul Woo[1] and Kyong-Tai Kim[1,3,*]

[1]Department of Life Science, Division of Molecular and Life Science, [2]School of Interdisciplinary Bioscience and Bioengineering and [3]Division of Integrative Bioscience & Biotechnology, Pohang University of Science and Technology, Pohang, Gyeong-Buk, 790-784, Republic of Korea

Received December 7, 2009; Revised June 22, 2011; Accepted July 7, 2011

ABSTRACT

Daily mRNA oscillations of circadian clock genes largely depend on transcriptional regulation. However, several lines of evidence highlight the critical role of post-transcriptional regulation in the oscillations of circadian mRNA oscillations. Clearly, variations in the mRNA decay rate lead to changes in the cycling profiles. However, the mechanisms controlling the mRNA stability of clock genes are not fully understood. Here we demonstrate that the turnover rate of mouse *Period3* (m*Per3*) mRNA is dramatically changed in a circadian phase-dependent manner. Furthermore, the circadian regulation of m*Per3* mRNA stability requires the co-operative function of 5′- and 3′-untranslated regions (UTRs). Heterogeneous nuclear ribonucleoprotein Q (hnRNP Q) binds to both 5′- and 3′-UTR and triggers enhancement of translation and acceleration of mRNA decay. We propose the phase-dependent translation coupled mRNA decay mediated by hnRNP Q as a new regulatory mechanism of the rhythmically regulated decay of m*Per3* mRNA.

INTRODUCTION

Circadian rhythms are daily physiological and behavioral oscillations observed in a variety of organisms. Circadian oscillations are driven by self-sustained time-keeping systems which are the intracellular clocks (1,2). These intracellular clocks consist of interacting positive and negative transcriptional and translational feedback loops of the clock genes (3–6). Daily oscillations in protein and/or mRNA levels are central features of the circadian genes (2,6). As for the underlying mechanism of mRNA cycling, a number of studies have shown that the oscillations of circadian genes are controlled at the transcriptional level (4,7–11). In Drosophila, nevertheless, it has been suggested that post-transcriptional regulations also contribute to the mRNA cycling (12–15). Furthermore, we previously demonstrated that 3′-untranslated region (UTR)-mediated mRNA decay played an essential role in m*Per3* mRNA cycling, providing direct evidence for the post-transcriptional control of circadian mRNA oscillation (16).

As the quantity of mRNA is ultimately reflected to the amount of translated protein, the regulation of mRNA half-life is considered to be an important control point in gene expression. During the past decades, a large number of studies have identified *cis*-acting elements and *trans*-acting factors involved in the regulation of mRNA stability (17–21), and showed that the turnover rates of mRNAs could be regulated by internal or external stimuli, such as cytokines, hormones, hypoxia, or viral infection (17,22–24). Recently, it was reported that the circadian clock regulates the stability of CCR-LIKE(CCL) mRNA, one of the clock-controlled genes of Arabidopsis (25).

Variations in mRNA stability clearly lead to changes in the mRNA cycling profiles of circadian genes (16), however, little is known about the mechanisms controlling the half-lives of mRNA. To investigate the underlying mechanisms, we established several lines of stably transformed NIH3T3 cells that express *luciferase* (Luc) mRNA with the UTRs (5′-UTR or/and 3′-UTR) of m*Per3* mRNA. Since many studies have shown that fibroblast cell lines, such as NIH3T3 and Rat-1, also contain an intrinsic circadian clock system, these cells have been used as

*To whom correspondence should be addressed. Tel: +82 54 279 2297; Fax: +82 54 279 2199; Email: ktk@postech.ac.kr
Present address:
Eunyee Kwak, Earlogic Auditory Research Institute, Seoul, Republic of Korea.
Kyung-Chul Woo, Newlife group Korean Research Institute for Skin Science, Sampoongdong 300 GB Technopark Global venture bld. #2201, Gyeongsan, Gyeong-Buk, Republic of Korea

The authors wish it to be known that, in their opinion, the first two authors should be regarded as joint First Authors.

appropriate experimental models to study the molecular mechanisms of the mammalian circadian clock (26–29).

Here, we present that the stability of mouse *Period3* (m*Per3*) mRNA, one of the mammalian circadian genes, is dramatically changed in a circadian phase-dependent manner. Furthermore, hnRNP Q has a critical role for the robust mRNA oscillation of m*Per3* and its translation. We suggest that the phase-dependent translation-coupled mRNA decay is involved in the regulation of the mRNA levels and oscillation pattern of m*Per3*. We demonstrate, for the first time in the field of circadian rhythm, that the cooperative function of the 5′- and 3′-UTRs is necessary and hnRNP Q plays a critical role in maintenance of the circadian oscillation of clock genes.

MATERIALS AND METHODS

Plasmids

A two-step PCR was performed to generate the promoter/5′-UTR/luciferase (Luc)/3′-UTR/neomycin (Neo) vector. The fragment containing the m*Per3* promoter region (4) and the 5′-UTR (accession no. NM_011067, version 1) was amplified from mouse (C57BL/6) genomic DNA with the forward primer (5′-CGGGGTACCCGCGCGT TATGTAAGGTACTCGGGGGCCTT-3′) and the reverse primer (5′-TTTGGCGTCTTCCATCCCGCCTG GCAGCCCTCAGCC-3′). The other fragment containing the N-terminus of the Luc-coding sequence was amplified from the pGL3 control vector (Promega) with the forward primer (5′-GGGCTGCCAGGCGGGATGGAAGACGC CAAAAACATAAAG-3′) and the reverse primer (5′-ATT TGTATTCAGCCCATATCG-3′). The second PCR fragment was digested with KpnI/NarI, cloned into the corresponding sites of the pGL3/3′-UTR vector (16), and designated as the promoter/5′-UTR/Luc/3′-UTR vector. The Neo-resistance gene preceded by the thymidine kinase promoter was amplified from the pMC1neo poly(A) vector (Stratagene) with the forward primer (5′-G CTCTAGAGCAGTGTGGTTTTGCAAGAGGAA-3′) and the reverse primer (5′-CAGGTCGACGGATCCGA ACAAACG-3′). Following XbaI/SalI digestion, the fragment was cloned into the corresponding sites of the promoter/5′-UTR/Luc/3′-UTR vector.

To generate the promoter/5′-UTR/Luc/Neo vector, the SV40 poly(A) signal was amplified from the pGL3 control vector (Promega) with the forward primer (5′-GCGAATT CCGGCCGCTTCGAGCAGACATGAT-3′) and the reverse primer (5′-GCTCTAGATACCACATTTGTAG AGGTTTTAC-3′), and digested with EcoRI/XbaI. The m*Per3* 3′-UTR from the promoter/5′-UTR/Luc/3′-UTR vector was removed by digestion with EcoRI/XbaI and replaced with the SV40 poly(A) signal, to form the promoter/5′-UTR/Luc/SV40 poly(A) vector. Following XbaI/SalI digestion, the Neo-resistance gene was cloned into the restriction sites.

To generate Per3 1–357/NAT, the m*Per3* 5′-UTR was amplified with the forward primer (5′-CCCAAGCTTCCC GCACGGCCGGGCGCTGCT-3′) and the reverse primer (5′-CGCGGATCCCCCGCCTGGCAGCCCTCA GCC -3′) from mouse suprachiasmatic nuclei cDNAs. To generate serial deletion constructs, m*Per3* 5′-UTR fragments were amplified with forward primers 5′-CCCAAG CTTGCTGACCGCGCTCCCTGAGAGC-3′ for Per3 120–357/NAT, 5′-CCCAAGCTTCTCAGATGAGCGT GGTCGGCG-3′ for Per3 240–357/NAT, and the reverse primer 5′- CGCGGATCCCCCGCCTGGCAGCCCTCA GCC -3′ for both of deletion constructs. The amplified fragment was digested with HindIII/BamHI, and cloned into the corresponding sites upstream of the arylalkylamine *N*-acetyltransferase (AANAT) coding sequence of the pcNAT control vector. To generate SL-5UTR-NAT, stem-loop oligonucleotide (5′-AGCTT GCCTAGGCCGGAGCGCCCAGATCTGGGCGCTC CGGCCTAGGCA-3′) was annealed to form a duplex. After poly nucleotide kinase treatment, it was was attached by ligase to Per3 1–357/NAT construct which was cut with HindIII.

To generate 5′-UTR-firefly Luc (FLUC), the pCY2 vector was modified (30). *Renilla* Luc (RLUC) and the intergenic sequences were removed by cutting with HindIII/XbaI, and the 5′-UTR of m*Per3* was ligated into the restriction enzyme sites. For *in vitro* binding followed by UV crosslinking, full-length and deletion fragments of the m*Per3* 5′-UTR were amplified as described above. The PCR products were digested with EcoRI and XbaI, and then inserted into the pSK′ vector (31), yielding pSK′ Per3 1–357, pSK′ Per3 120–357, pSK′ Per3 240–357.

Cell culture and generation of stable cell lines

The NIH3T3 cell line was maintained in Dulbecco's modified Eagle's medium (DMEM) supplemented with 10% fetal bovine serum and 1% penicillin–streptomycin in a humidified atmosphere containing 5% CO_2 at 37°C.

To generate the NIH-m*Per3* promoter-5′-UTR-Luc-3′-UTR and NIH-m*Per3* promoter-5′-UTR-Luc stable cell lines, the promoter/5′-UTR/Luc/3′-UTR/Neo and promoter/5′-UTR/Luc/Neo vectors were introduced to NIH3T3 fibroblasts by using the calcium phosphate precipitation method, respectively. After 2 days, we started selection with 800 μg G418/ml (Invitrogen). Neomycin-resistant clones were isolated by the standard procedure. The resulting cell lines were maintained in DMEM supplemented with 10% bovine calf serum, 1% penicillin–streptomycin and 200 μg G418/ml.

Dexamethasone shock and mRNA decay kinetics

The dexamethasone shock was done as previously described (16). In brief, $\sim 1.5 \times 10^5$ cells/well were seeded in 12-well plates. When the cells reached confluence, the medium was exchanged with a medium containing 100 nM dexamethasone. After 2 h, this medium was replaced with complete medium. To examine the mRNA oscillation profiles, cells were harvested at the indicated times and stored at −70°C until total RNA was extracted.

To examine the mRNA decay kinetics in the rising phase, actinomycin D was added to a final concentration of 5 μg/ml after 18 h of dexamethasone shock. At the indicated time, the cells were harvested and kept at −70°C until total RNA was extracted. For mRNA

decay kinetics in the declining phase, actinomycin D was added after 30 h of dexamethasone shock.

In vitro RNA synthesis and the luciferase assay

For mRNA transfection, 5′-UTR-FLUC was linearized by digestion with EcoRI. This plasmid contains a 20-nt long poly (A) sequence upstream of the EcoRI site. Reporter mRNA was *in vitro* transcribed with SP6 RNA polymerase (Roche) in the presence of the cap analog. The RLUC control mRNA reporter was linearized by digestion with XbaI. Firefly and *Renilla* Luc activities were determined using the Dual-Luciferase Reporter Assay System (Promega) according to the manufacturer's instructions.

Transient transfection and the AANAT assay

For plasmid transfection, cells were seeded in 24-well plates at a density of 1.0×10^5 cells/well a day prior to transfection. Transfection was carried out using Metafectene (Biontex) according to the manufacturer's instructions. After incubation for 24 or 36 h, cells were harvested for further experiments. For mRNA transfection, NIH3T3 cells were seeded in 24-well plates at a density of 1.0×10^5 cells/well on the day prior to synchronization. We transfected 2 μg of capped reporter mRNA into NIH3T3 cells at the indicated time points using Lipofectamine 2000 (Invitrogen) according to the manufacturer's instructions. After incubation for 6 h, the cells were harvested for further experiments.

AANAT activity was determined as previously described (32). In brief, the transfected cells were disrupted by five times of freezing and thawing cycle. After centrifugation, the supernatant was incubated in the presence of 2.5 mM tryptamine–HCl, 25 μM acetyl CoA and 1 μl [^{3}H] acetyl CoA (3.6 Ci/mmol, 250 μCi/ml) at 37°C for 30 min. The reaction was stopped by dilution with 50 mM sodium phosphate buffer. The amount of radiolabeled acetyltryptamine was determined using a liquid scintillation counter.

Quantitative Real-time RT–PCR

Quantitative real-time RT–PCR was performed as previously described (16). In brief, total RNA was isolated by using the TRI Reagent (Molecular Research Center). RNA was reverse transcribed by using Moloney murine leukemia virus reverse transcriptase (Roche Applied Science) according to the manufacturer's instructions. For detection and quantification, the MyiQ™ Real-Time PCR Detection System (Bio-Rad) was used. The sequences of the forward and reverse primers were as follows: endogenous m*Per3*, 5′-TTGTCAGGTTGGC CTTCTCT-3′ and 5′-GGCATCCTAGCAGAGGTG AG-3′; Luc, 5′-GAGGTTCCATCTGCCAGGTA-3′ and 5′-CACACAGTTCGCCTCTTTGA-3′; mouse TATA-binding protein (mTBP), 5′-CAGCCTTCCACCT TATGCTC-3′ and 5′-TTGCTGCTGCTGTCTTTG TT-3′; mouse ribosomal protein L32 (mRPL32), 5′-AAC CCAGAGGCATTGACAAC-3′ and 5′-CACCTCCAGC TCCTTGACAT-3′; rAANAT, 5′-TTTGAGATTGAGC GCGAAG-3′ and 5′-TCGAACCAGCCCAGTGAC-3′

Real-time bioluminescence monitoring

A total of 5.0×10^5 cells were plated into 35-mm culture dishes. When the cells reached confluence, the medium was exchanged with medium containing 100 nM dexamethasone. After 2 h, this medium was replaced with complete medium supplemented with 50 mM HEPES (pH 7.2) and 0.1 mM luciferin (Promega). Cultures were maintained at 37°C and bioluminescence was monitored continuously using an AB-2500 Kronos luminometer (Atto Corporation). Photon counts were integrated over 1-min intervals.

RNA interference

The sequences of synthesized siRNAs were as follows. siCon: 5′-UUCUCCGAACGUGUCACGUTT-3′ (Samchully Pharm.), sihnRNP Q: 5′-AGACAGUGAUC UCUCUCAUTT-3′ (Dharmacon Research). For siRNA transfection into NIH3T3 cell lines, a microporator (Digital-Bio) was used, according to the manufacturer's instructions.

Protein preparation and immunoblot analysis

For immunoblotting, cells were disrupted with complete protein solubilizing buffer containing 1% SDS and M urea in PBS, followed by sonication. Fractionation of NIH3T3 cells into cytosolic extracts was performed as described (30). Immunoblot analyses were performed with monoclonal anti-14-3-3ξ (Santa Cruz), polyclonal antibody against hnRNP Q (Sigma-Aldrich). HRP-conjugated mouse, rabbit (KPL) or rat (Santa Cruz) secondary antibodies were detected with SUPEX ECL reagent (Neuronex) and a LAS-4000 system (FUJI FILM), according to the manufacturer's instructions.

In vitro binding assay and immunoprecipitation

In vitro binding assay was performed as described previously (30). In brief, XbaI-linearized pSK′-5′-UTR constructs were transcribed using T7 RNA polymerase (Promega) in the presence of [α-32P] UTP. Twenty micrograms of nuclear extracts or 40 μg of cytosolic extracts were incubated with labeled RNAs at 30°C. After 30 min of incubation, the mixtures were UV-irradiated on ice for 15 min with a CL-1000 UV-crosslinker (UVP). The samples were detected with autoradiography after SDS–PAGE. To confirm the identity of the UV cross-linked protein, 3 μg of a polyclonal antibody against hnRNP Q or pre-immune serum were added to RNase-digested reaction mixtures. After 16 h, Protein G agarose beads (Amersham bioscience) were added. After a further incubation for 3 h, precipitates were detected with autoradiography after SDS–PAGE.

RESULTS

m*Per3* mRNA stability is regulated in a circadian phase-dependent manner

In circadian phase-synchronized NIH3T3 fibroblasts, endogenous m*Per3* mRNA levels began to increase after 18 h of dexamethasone treatment and decreased after reaching

their peak levels between 24 and 30 h (Figure 1A). To examine whether m*Per3* mRNA stability was regulated by circadian rhythm, we analyzed the mRNA decay kinetics in the circadian phase-synchronized NIH3T3 cells. To compare the decay kinetics of the rising phase or the declining phase, transcription was blocked with actinomycin D at 18 or 30 h after dexamethasone shock, respectively. As shown in Figure 1B and Supplementary Figure S1, m*Per3* mRNA stability was dramatically regulated in a circadian phase-dependent manner. m*Per3* mRNA was very stable in the rising phase (especially during the first 2 h), whereas it was rapidly degraded in the declining phase. To explore the specificity of these results, we then analyzed the decay kinetics of TBP mRNA, whose levels are constant, irrespective of circadian rhythm (27). As expected, TBP mRNA decay kinetics was not altered during circadian rhythm (Figure 1C) in contrast to the m*Per3* mRNA. Based on these results, we concluded that m*Per3* mRNA stability is regulated by circadian rhythm and that the circadian control of mRNA stability is a specific phenomenon that is restricted to a subset of mRNAs.

3′-UTR-mediated mRNA decay is necessary but not sufficient for the circadian control of m*Per3* mRNA stability

To examine whether the m*Per3* mRNA oscillation pattern was regulated with only transcriptional control, we established NIH-m*Per3* promoter-Luc stable cell lines that express the luciferase gene under the control of the wild-type m*Per3* promoter without any UTRs. Surprisingly, the total amount of reporter mRNA increased gradually after phase-synchronization with dexamethasone. Although it seemed to show a 24-h period oscillation pattern to some degree, a breakdown of the mRNA level balancing mechanism could be a

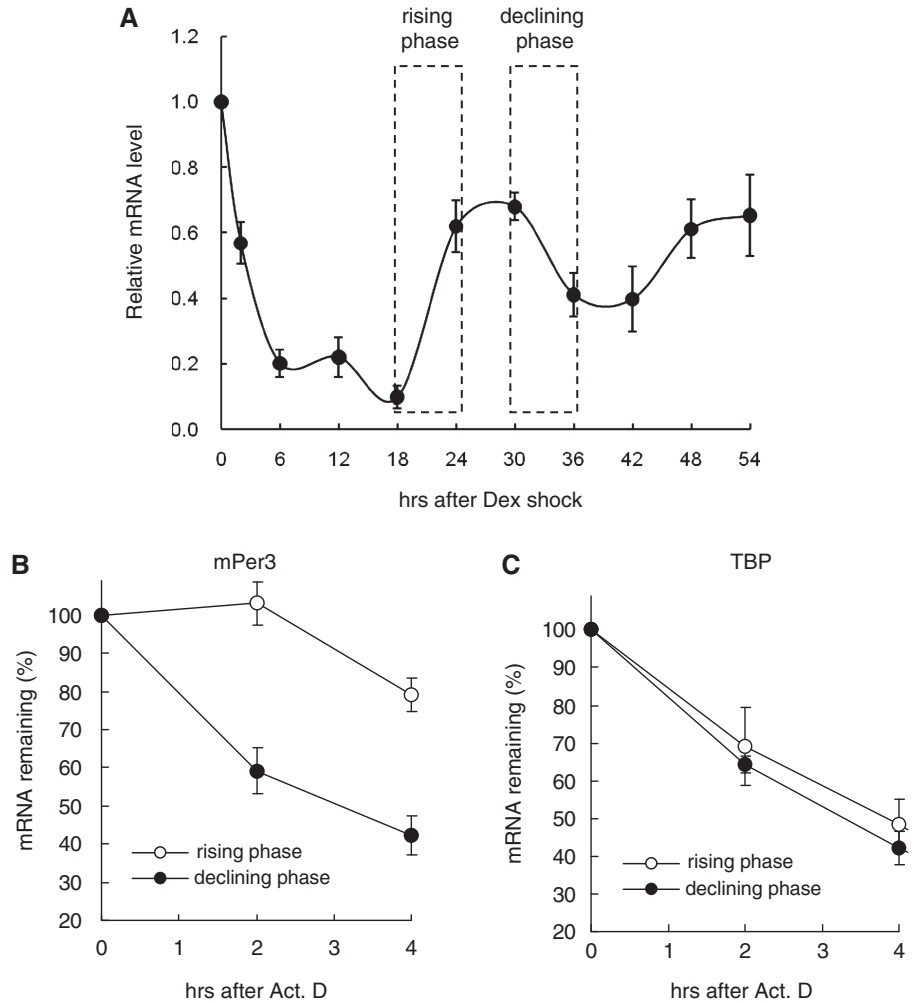

Figure 1. Circadian rhythm regulates m*Per3* mRNA stability. (**A**) Endogenous m*Per3* mRNA oscillation pattern was confirmed. For the decay kinetics of the rising or declining phases, transcription was blocked after 18 or 30 h of dexamethasone treatment, respectively. Both of rising and declining phases were indicated. (**B**) mRNA decay analyses were performed as mentioned in Materials and methods section. Decay kinetics of endogenous m*Per3* mRNA from circadian phase-synchronized NIH3T3 fibroblasts with dexamethasone treatment are shown. The m*Per3* mRNA levels were determined by quantitative real-time RT–PCR and normalized to RPL32 mRNA levels. (**C**) Decay kinetics of TBP mRNA from circadian phase-synchronized NIH3T3 fibroblasts with dexamethasone treatment are shown. The TBP mRNA levels were determined by quantitative real-time RT–PCR and normalized to RPL32 mRNA levels. All results are presented as the mean ± SD of three experiments.

potential obstacle in cellular homeostasis (Figure 2A). In the m*Per3* promoter-Luc stable cell lines, the reporter mRNA was also transcribed by a D box element within the wild-type m*Per3* promoter; nevertheless, the reporter mRNA showed a continuously accumulating pattern. In that case, it is possible that the decay of the reporter mRNA was less active in the NIH-m*Per3* promoter-Luc stable cell lines. As expected, the mRNA degradation kinetics of the UTR-free reporter was much slower than that of UTR-bearing endogenous m*Per3* mRNA (Figure 2B). Moreover, we did not observe a phase-dependency of mRNA decay.

Previously, we established NIH-Luc-WT 3′-UTR stable cell lines that produce mRNA of the Luc coding region followed by the 3′-UTR of the wild-type m*Per3*, and showed that the m*Per3* 3′-UTR is necessary for circadian mRNA oscillations (16). To examine whether m*Per3* 3′-UTR-mediated mRNA decay is sufficient for the circadian control of mRNA stability, we analyzed the decay kinetics of Luc mRNA containing the m*Per3* 3′-UTR after blocking transcription. As shown in Figure 2D, although the reporter mRNA was a little more stable in the rising phase than in the declining phase, the m*Per3* 3′-UTR alone could not reproduce the dramatic changes of mRNA decay kinetics as shown for the endogenous m*Per3* mRNA. The reporter mRNA oscillation profile showed an ~6-h phase delay compared to endogenous m*Per3* mRNA (Figure 2C) (16). According to these results, we concluded that the contribution of the m*Per3* 3′-UTR alone is not sufficient to replicate the endogenous oscillation pattern of m*Per3* mRNA. Therefore, we needed to analyze the role of the m*Per3* 5′-UTR in mRNA decay regulation.

The m*Per3* 5′-UTR mediates translational regulation-coupled mRNA decay

Although a large number of studies have demonstrated 5′-UTR-mediated translational regulation (33,34), several studies also reported that mRNA stability could be regulated by the 5′-UTR, a mechanism called translational regulation-coupled mRNA decay. In such cases, translational inhibition caused mRNA stabilization (35–39).

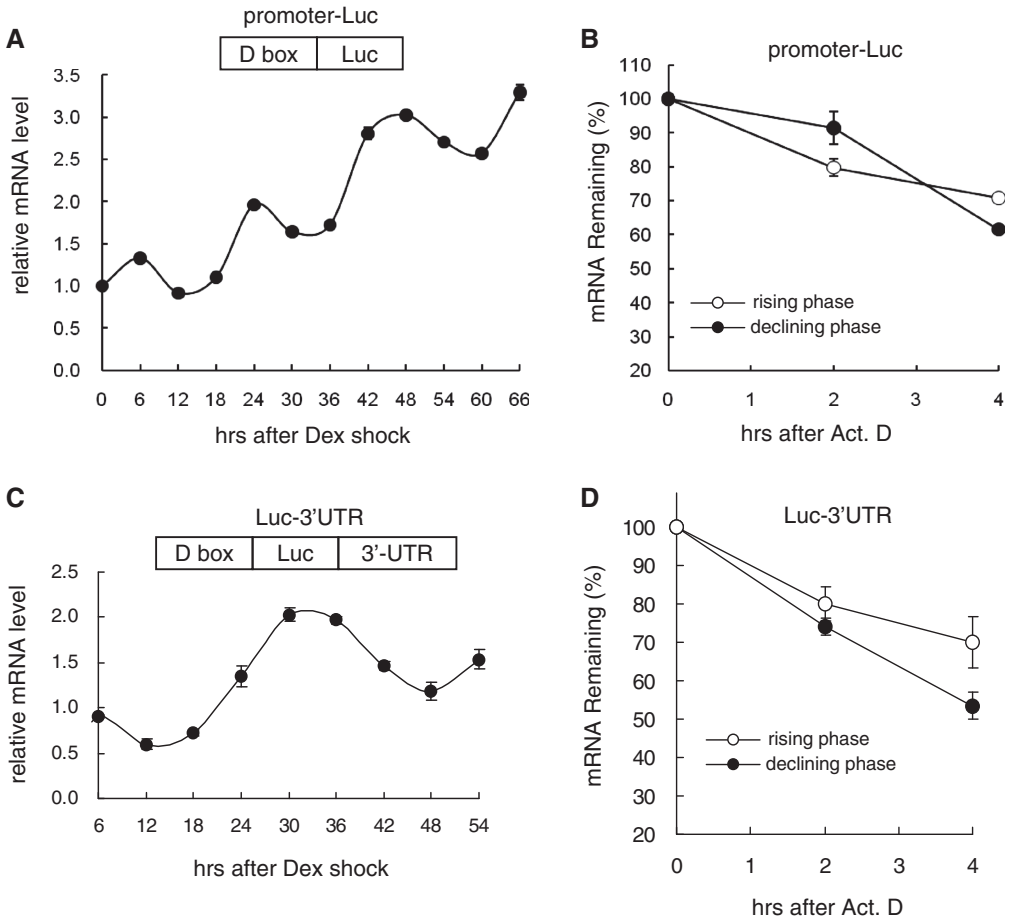

Figure 2. The m*Per3* 3′-UTR is necessary but not sufficient for the circadian control of mRNA stability. (**A** and **C**) Temporal expression profiles of luciferase (Luc) mRNA without a UTR (A) or with the m*Per3* 3′-UTR (C) are shown from NIH-m*Per3* promoter-Luc stable cells (A) or NIH-Luc-WT 3′-UTR stable cells (C) after circadian phase-synchronization with dexamethasone treatment. Schematic diagrams of reporter genes expressed in each cell lines are shown. When dexamethasone was added, the time was set to 0. Reporter mRNA levels were determined by quantitative real-time RT–PCR and normalized to TBP mRNA levels. The initial level of reporter mRNA was arbitrarily set to 1.0. (**B** and **D**) Decay kinetics of Luc mRNA without a UTR (B) or with the m*Per3* 3′-UTR (D) are shown. The reporter mRNA levels were determined by quantitative real-time RT–PCR and normalized to RPL32 mRNA levels. All results are presented as the mean ± SD of three experiments.

To test whether this mechanism also exists in the regulation of the levels of m*Per3* mRNA, we cloned a reporter construct by inserting the wild-type m*Per3* 5′-UTR upstream of serotonin *N*-acetyltransferase (AANAT) coding region (Per3 1–357/NAT) (32). We also prepared the other construct that had a stem-loop structure at the upstream of the m*Per3* 5′-UTR in 5UTR-NAT reporter to block the ribosome scanning (SL-Per3 1–357/NAT) (Figure 3A). The effect of this structure on translation was analyzed by transient transfection followed by measurement of AANAT activity. As expected, the stem-loop-harboring construct showed lower AANAT activity than the wild-type construct, even though reporter mRNA level was elevated due to higher transfection efficiency (Figure 3B). This result indicated that the stem–loop structure could inhibit the translation of downstream gene efficiently. Interestingly, the construct with a lower translation rate showed a slower mRNA decay rate (Figure 3C). This reciprocal relationship between translation efficiency and mRNA stability suggests that the m*Per3* 5′-UTR mediates a coupling between translation and mRNA decay.

Increasing evidence has suggested that upstream open reading frames (uORFs) can regulate their mRNA translation. m*Per3* has four uORFs within the m*Per3* 5′-UTR, including one overlapping uORF. To determine the potential role of these uORFs, we generated four single-nucleotide mutant constructs in which AUG was changed to AAG (Per3 uAUG-1 mut/NAT, Per3 uAUG-2 mut/NAT, Per3 uAUG-3 mut/NAT, Per3 uAUG-4 mut/NAT). The effects of these mutations on translation were analyzed by transient transfection and the reporter, AANAT assay. However, we could not observe any differences in AANAT level between WT and mutant constructs (Supplementary Figure S4A). In addition, mRNA decay kinetics of WT and mutant reporters were comparable (Supplementary Figure S4B). Therefore, we concluded that uORF-mediated translation regulation is not crucial step in the case of m*Per3*.

Circadian control of m*Per3* mRNA stability requires the cooperative function of the 5′- and 3′-UTRs

Since m*Per3* mRNA stability was regulated in a circadian phase-dependent manner, we hypothesized that m*Per3*

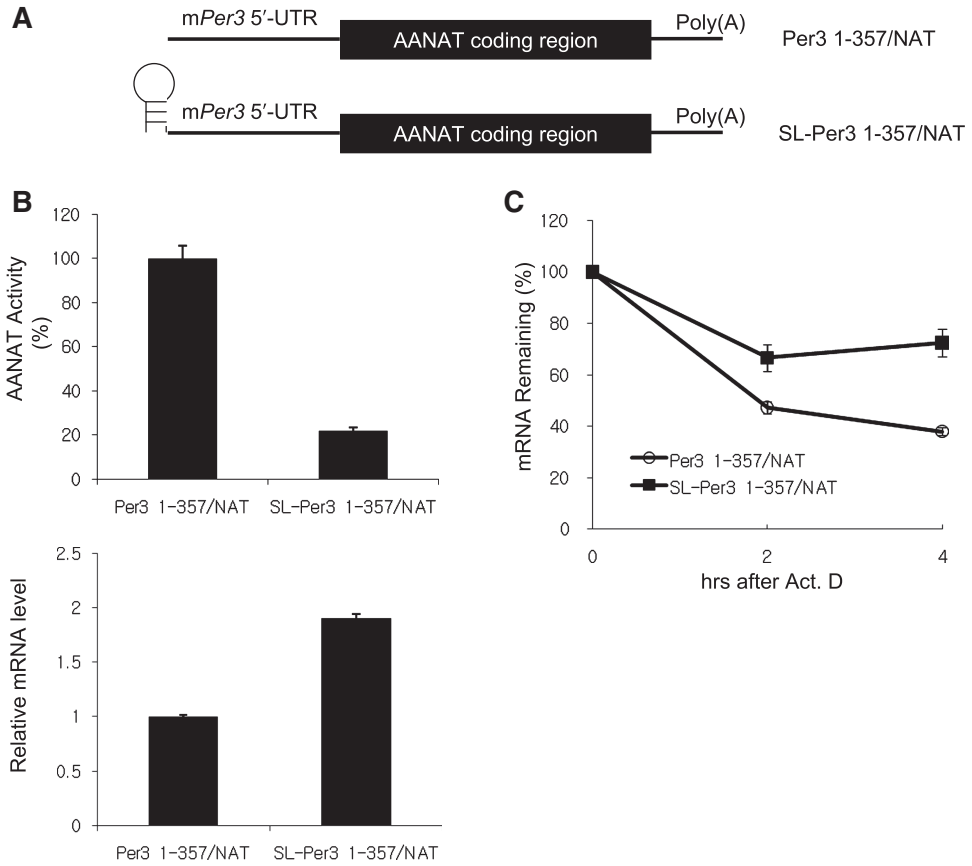

Figure 3. The m*Per3* 5′-UTR mediates translation-mRNA decay coupling. (**A**) Schematic diagrams of pcNAT reporters. m*Per3* 5′-UTR with (SL-Per3 1–357/NAT) or without (Per3 1–357/NAT) stem–loop structure was fused to the AANAT coding region. (**B**) Translation efficiency of each pcNAT reporter was measured by the AANAT assay. An amount of 0.5 μg of each construct was transiently transfected into HEK293A cells. The AANAT assay was performed 24 h after transfection. The AANAT level in Per3 1–357/NAT reporter transfected cells was arbitrarily set to 100 (upper panel). The reporter transcript level of each construct was determined using quantitative RT–PCR, and normalized to RPL32 mRNA levels (lower panel). (**C**) The decay kinetics of AANAT mRNA expressed from each reporter are shown. Cells were treated with 5 μg/ml actinomycin D, 24 h after transfection of each reporter. All results are representative of at least three independent experiments. The error bars represent the mean ± SEM of duplicate measurements.

translational regulation-coupled mRNA decay would also be rhythmically regulated. To confirm the hypothesis, we compared the decay rate of endogenous m*Per3* mRNA between the translation-inhibited condition and the normal condition in both the rising and declining phases in phase-synchronized NIH3T3 mouse fibroblasts. Interestingly, m*Per3* mRNA was more stable when both transcription and translation were blocked by actinomycin D and cycloheximide treatment, respectively, than only when transcription was blocked. Moreover, this phenomenon was more dramatic in the declining phase when m*Per3* mRNA decay was accelerated (Figure 4A). This result suggests that translation-mRNA decay coupling may occur differentially, dependent on the mRNA oscillation phase.

However, upregulation of m*Per3* mRNA stability by cycloheximide treatment could result from the synthesis blockade of proteins that promote the clearance of m*Per3* mRNA. To exclude this possibility, two cap-harboring mRNA reporters were generated by *in vitro* transcription: the 5′-UTR-FLUC (firefly luciferase) reporter, composed of the mPer3 5′-UTR followed by FLUC, and the RLUC reporter which contains only RLUC (Renilla luciferase) coding sequence. Two mRNA reporters were transiently co-transfected into phase-synchronized NIH3T3 fibroblasts at 18 or 28 h after dexamethasone shock. Six hours later, translated FLUC and RLUC levels were analyzed by the luciferase assay. RLUC level which determined the transfection efficiency was slightly decreased in 28–34 h after synchronization than in 18–24 h. Nevertheless, the 5′-UTR-FLUC transcript was ~1.5-fold more translated in the m*Per3* mRNA decay-favoring declining phase than in the rising phase (Figure 4B). This result suggests that m*Per3* 5′-UTR-mediated translation is also rhythmically regulated.

Since 3′-UTR-mediated mRNA decay was not sufficient to reproduce the phase-dependent mRNA stability changes of m*Per3* and we identified that the 5′-UTR was also involved in the mRNA decay process, we established NIH-m*Per3* promoter-5′-UTR-Luc-3′-UTR stable cell lines that express Luc mRNA containing both the 5′- and 3′-UTRs of m*Per3* mRNA upstream and downstream of the Luc coding sequences, respectively. Interestingly, the Luc mRNA with both the 5′- and 3′-UTRs of m*Per3* (i.e. 5′-UTR-Luc-3′-UTR) oscillated similarly to the endogenous m*Per3* mRNA (Figure 4C). The notable thing is that the decay kinetics of this reporter mRNA were nearly the same as the endogenous m*Per3* mRNA (Figure 4D). This result suggests that the cooperative functions of the 5′- and 3′-UTRs are necessary for the circadian control of the decay rate of m*Per3* mRNA.

As shown in Figure 4E, the mRNA level was in the rising phase at 16 h after dexamethasone treatment and increased continuously to 26 h. Interestingly, the oscillation profile of Luc activity was very different from that of the reporter mRNA. Especially, in spite of rising mRNA levels, the protein levels decreased until ~21.5 h after dexamethasone treatment. As a result, a distinct phase-lag between the mRNA and protein levels was observed. This result supported our hypothesis that translation was inhibited during the early rising phase of mRNA levels and translational inhibition may induce the stabilization of the mRNA in the rising phase.

Downregulation of hnRNP Q not only reduces the translation efficiency but also increases the mRNA stability of m*Per3*

To identify the *cis*-acting region and trans-acting factors which are in charge of translation initiation and mRNA decay regulation, we performed *in vitro* binding assay followed by UV crosslinking with deletion constructs. While there was little change in protein binding pattern when the 5′ proximal 119 nt within the 5′-UTR of the m*Per3* mRNA were deleted (Per3 120–357), several proteins were dramatically dissociated when additional 120 nt were deleted (Per3 240–357) (Figure 5A). Previously, we reported that 68-kDa protein hnRNP Q bound to 5′-UTR of AANAT, the key enzyme in the melatonin biogenesis, and enhanced its translation kinetics (30). Also, we already identified that hnRNP Q could control the translation initiation of mRev-erb α in phase-dependent manner (40). In line with such findings, we discovered that 68-kDa protein showed dramatically reduced binding to the Per3 240–357 construct. As a result of *in vitro* binding assay with whole cell lysates from NIH3T3 cell lines that hnRNP Q was downregulated with siRNA, the binding of 68-kDa protein was markedly reduced and this protein was exactly the same size of hnRNP Q (Figure 5A). To confirm the interaction between hnRNP Q and m*Per3* mRNA, UV crosslinking followed by immunoprecipitation with antibodies against hnRNP Q was performed. Among several cellular proteins bound to radioisotope-labeled UTRs of m*Per3*, we confirmed that hnRNP Q was clearly bound to both 5′- and 3′-UTR of m*Per3*. In contrast, we could not detect any bands in precipitates using pre-immune serum (Figure 5B). The association between 5′-UTR of m*Per3* and hnRNP Q was confirmed by RNA affinity purification using biotin–streptavidin interaction followed by immunoblot analysis (Supplementary Figure S2).

To test whether a deficiency in hnRNP Q also affects the translation efficiency of m*Per3*, we transiently transfected either control siRNA or the siRNA against hnRNP Q (sihnRNP Q) into NIH3T3 cells. After 12 h, we additionally transfected the m*Per3* 5′-UTR-inserted pcNAT reporter (Per3 1–357/NAT) into siRNA-transfected NIH3T3 cells. The amount of translated proteins was measured by AANAT assay. Interestingly, translated protein level showed ~20% decrease in sihnRNP Q-transfected cells, compared to siCon-transfected cells (Figure 5C). Translational reduction in hnRNP Q-downregulated cells was also observed when 5′ proximal 119 nt within the 5′-UTR of the m*Per3* mRNA were deleted (Per3 120–357/NAT). However, there was little reduction in the AANAT level in hnRNP Q-knockdowned cells when 120 nt within the 5′-UTR of the m*Per3* mRNA were additionally removed (Per3 240–357/NAT). Reduction of hnRNP Q level was confirmed by western blotting (Figure 5C).

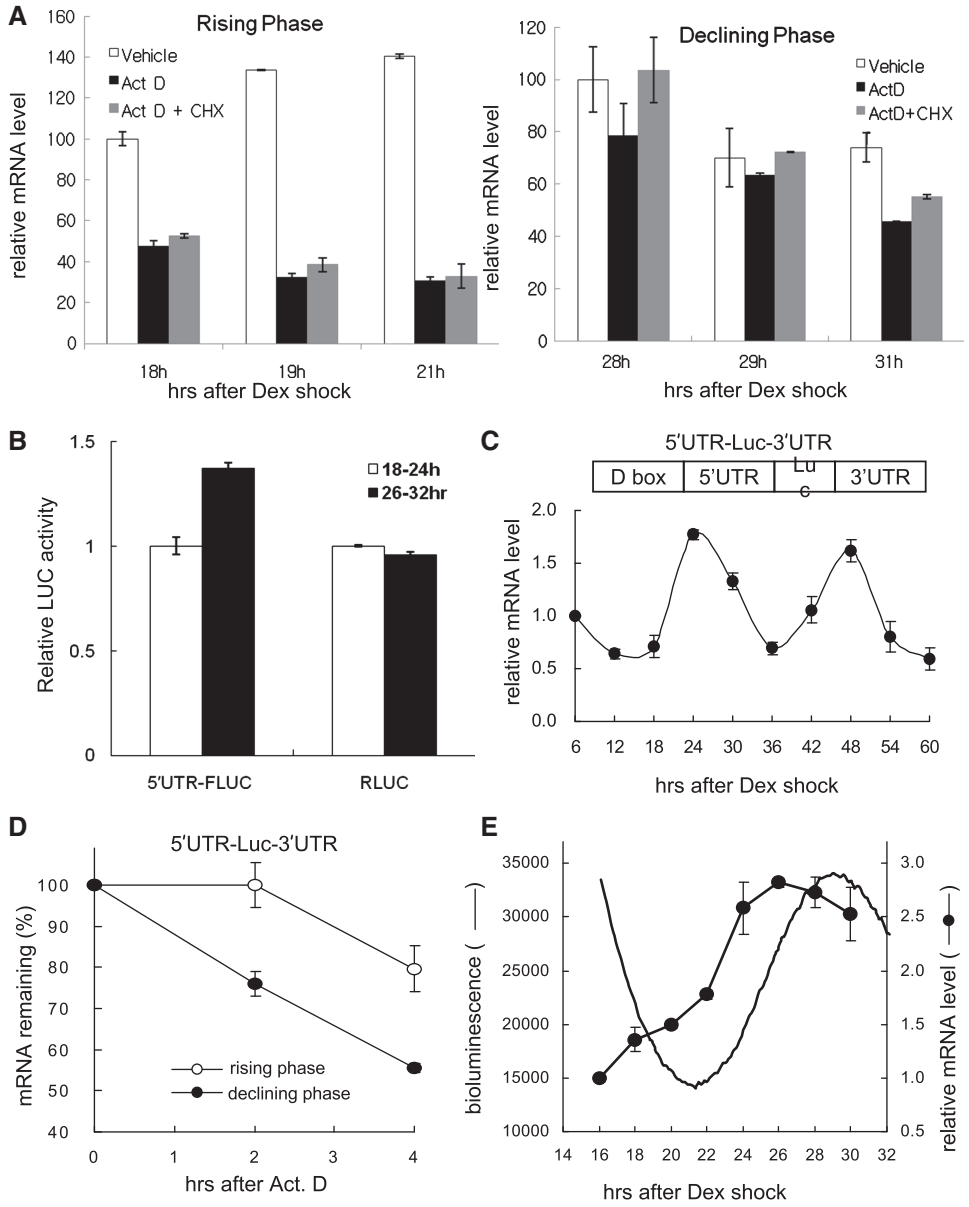

Figure 4. Circadian control of mPer3 mRNA stability requires the cooperative function of the 5′- and 3′-UTRs. (**A**) Phase-synchronized NIH3T3 fibroblasts were treated with vehicle, actinomycin D, or actinomycin D with 50 μg/ml cycloheximide at 17 h (rising phase) or 27 h (declining phase) after dexamethasone treatment. The endogenous m*Per3* mRNA levels were determined by quantitative real-time RT–PCR and normalized to RPL32 mRNA levels at the indicated time points. The initial level of m*Per3* mRNA (at 18 h in rising phase, at 28 h in declining phase) was arbitrarily set to 100. The results are presented as the mean ± SD of three experiments. (**B**) An amount of 2 μg of *in vitro* transcribed two mRNA reporters, 5′-capped 5′-UTR-FLUC or 5′-capped RLUC, were co-transfected at 18 or 28 h after synchronization. After 6 h, the luciferase assay was performed. The FLUC and RLUC level during 18–26 h after synchronization were set to 1.0. The error bars represent the mean ± SEM of duplicate measurements. (**C**) Temporal expression profiles of luciferase (Luc) mRNA with both the m*Per3* 5′- and 3′-UTRs are shown from NIH-m*Per3* promoter-5′-UTR-Luc-3′-UTR stable cells after circadian phase-synchronization with dexamethasone (Dex) treatment. Reporter mRNA levels were determined by quantitative real-time RT–PCR and normalized to TBP mRNA levels. The initial level of reporter mRNA was arbitrarily set to 1.0. (**D**) The decay kinetics of Luc mRNA with both the m*Per3* 5′- and 3′-UTRs are shown. The reporter mRNA levels were determined by quantitative real-time RT–PCR and normalized to the RPL32 mRNA levels. In (C) and (D), each point presented is the mean ± SD of three experiments. (**E**) Comparison of LUC mRNA and protein profiles. Real-time bioluminescence of NIH-m*Per3* promoter-5′-UTR-Luc-3′-UTR stable cells was monitored. The unit of bioluminescence (y-axis) is photons/min. Reporter mRNA levels were determined by quantitative real-time RT–PCR and normalized to the TBP mRNA levels.

Next, we sought to determine whether the decrease in reporter translation by downregulation of hnRNP Q could influence the stability of reporter mRNA. Consistent with the result of Figure 3, Per3 1–357/NAT and Per3 120–357/NAT transcripts were more stable when translation initiation was less active by sihnRNP Q-transfection. However, we could not observe any differences in the stability of Per3 240–357/NAT transcripts when hnRNP Q level was downregulated (Figure 5D), mirroring the results obtained from *in vitro* binding

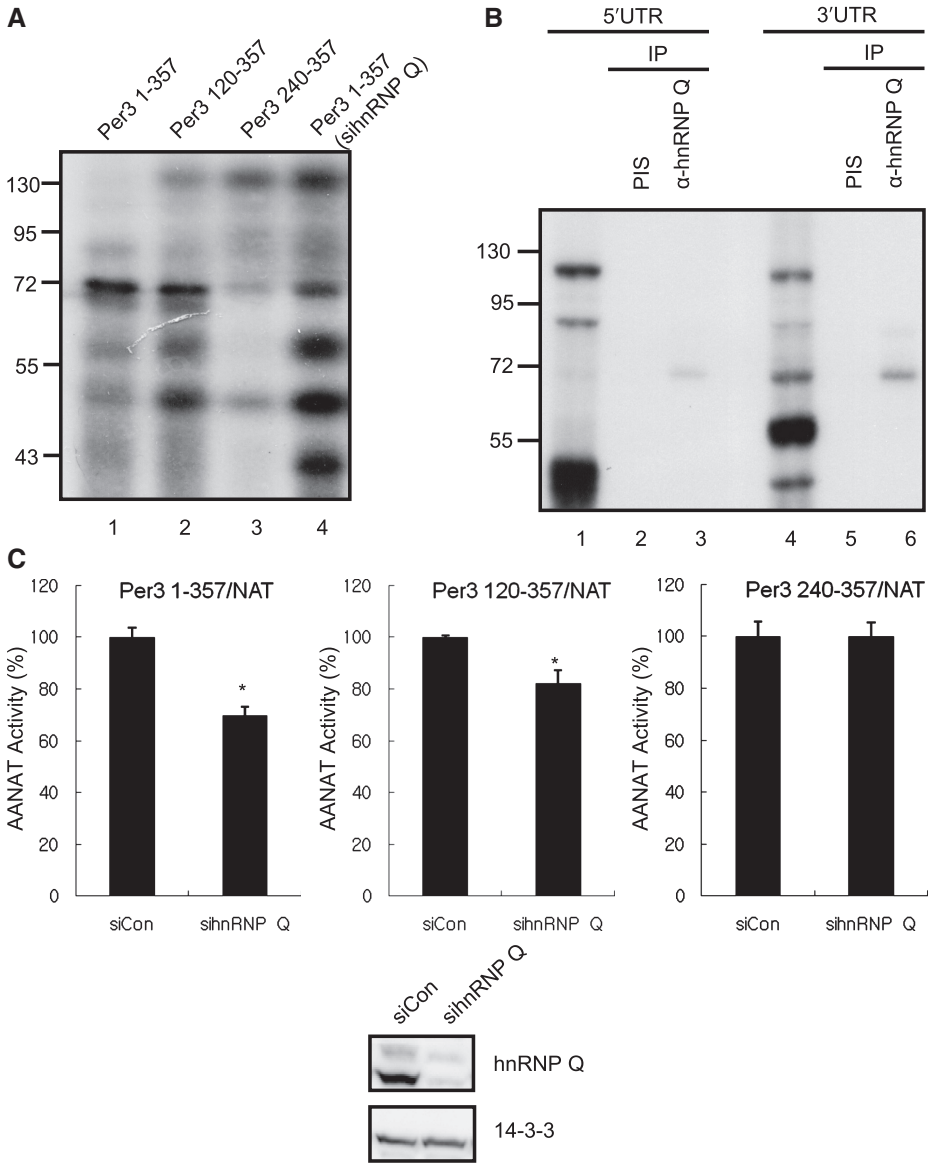

Figure 5. hnRNP Q regulates the translation-coupled mRNA decay of m*Per3*. (**A**) Cellular proteins that bound to the wild-type or truncated forms of m*Per3* 5′-UTR were analyzed with the *in vitro* binding followed by UV-crosslinking assay. Whole lysates were extracted from NIH3T3 cells (lane 1–3). Cellular proteins that bound to the full length of the m*Per3* 5′-UTR were analyzed. Whole lysates were extracted from NIH3T3 cells which hnRNP Q was downregulated (lane 4). The sizes of proteins are indicated to the left of the panels. (**B**) Identification the interaction between hnRNP Q and both UTRs of m*Per3*, using UV crosslinking followed by immunoprecipitation. In lane 1 and 4, cellular proteins that bound to the m*Per3* 5′-UTR (lane 1) or 3′-UTR (lane 4) were analyzed with the *in vitro* binding followed by UV-crosslinking assay. Cytoplasmic lysates were extracted from NIH3T3 cells. The sizes of proteins are indicated to the left of the panels. PIS, pre-immune serum. (**C**) Translation initiation controlled by wild-type or truncated forms of m*Per3* 5′-UTR is analyzed when the hnRNP Q is downregulated. Per3 120–357/NAT and Per3 240–357/NAT are deletion constructs of Per3 1–357/NAT. 0.5 μg of reporter plasmid was transiently transfected into NIH3T3 cell lines which were pre-transfected with either control siRNA (siCon) or siRNA against hnRNP Q (sihnRNP Q). Translation efficiency of AANAT reporter was measured by the AANAT assay. For transfection control, 0.1 μg of beta-galactosidase plasmid was cotransfected. The AANAT assay and beta-galactosidase assay were performed at 36 h after transfection. The normalized AANAT level in siCon-transfected cells was arbitrarily set to 100. The significance of differences of AANAT activities was determined by Student's *t*-test. $*P < 0.005$. (**D**) After co-transfection of 0.05 μg of AANAT reporter with either siCon or sihnRNP Q, the decay kinetics of the reporter mRNA was analyzed. Cells were treated with 5 μg/ml actinomycin D, at 18 h after co-transfection. Knockdown efficiency was confirmed by western blot. (**E**) After transfection with either siCon or sihnRNP Q, the decay kinetics of endogenous m*Per3* was analyzed. Cells were treated with 5 μg/ml actinomycin D, 24 h after siRNA-transfection. (D and E) Decay kinetics of TBP mRNA was analyzed for negative control. Each mRNA levels was determined by quantitative real-time RT–PCR and normalized to RPL32 mRNA levels. In (C) to (E), all results are representative of at least three independent experiments. The error bars represent the mean ± SD of duplicate measurements.

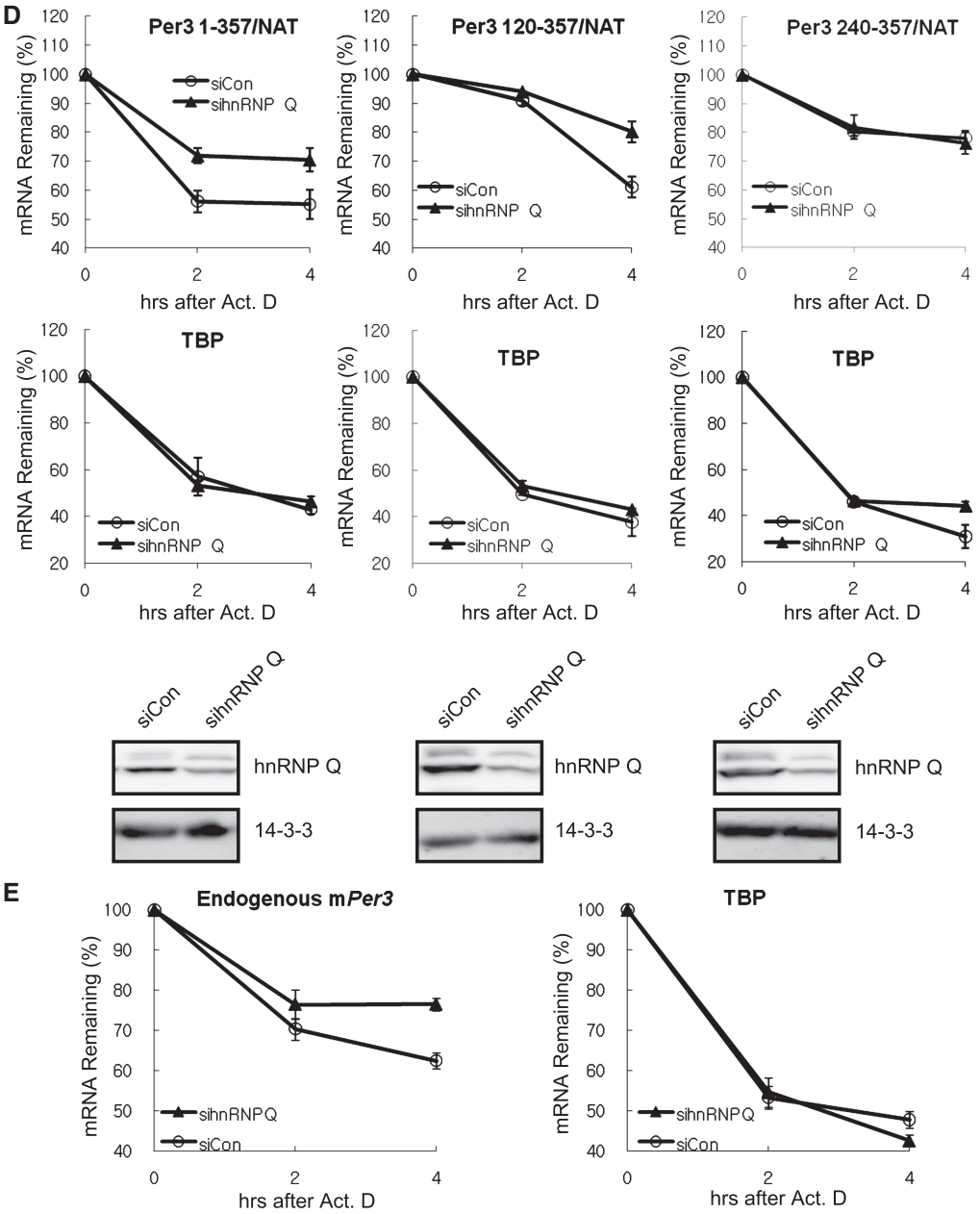

Figure 5. Continued.

assay and AANAT assay. Furthermore, the degradation kinetics of endogenous m*Per3* was also slower in sihnRNP Q-transfected condition than in siCon-transfected condition (Figure 5E). To determine the specificity of hnRNP Q downregulation effect, we exogenously expressed hnRNP Q in endogenous hnRNP Q-downregulated cells. As a result, altered mRNA decay kinetics of m*Per3* by hnRNP Q knockdown was rescued by exogenous hnRNP Q expression (Supplementary Figure S3A). However, the degradation kinetics of endogenous TBP mRNA was not altered in all conditions (Figure 5D, E and Supplementary Figure S3B). These results supported that the m*Per3* mRNA decay was connected to its translation kinetics and the central region of m*Per3* 5′-UTR (120–239 nt) was responsible for coupling of translation and mRNA decay. Moreover, hnRNP Q was strong candidate in this regulatory mechanism.

hnRNP Q binds to 5′-UTR of m*Per3* in a phase-dependent manner, and maintains the robust mRNA oscillation

Since both translation and mRNA decay are more active in the declining phase and hnRNP Q was concerned with those events, we hypothesized that the binding affinity of hnRNP Q to 5′-UTR of m*Per3* would be higher in the declining phase than in the rising phase. Based on the general knowledge that a translation occurs in the cytoplasm, we analyzed the phase-dependent interaction

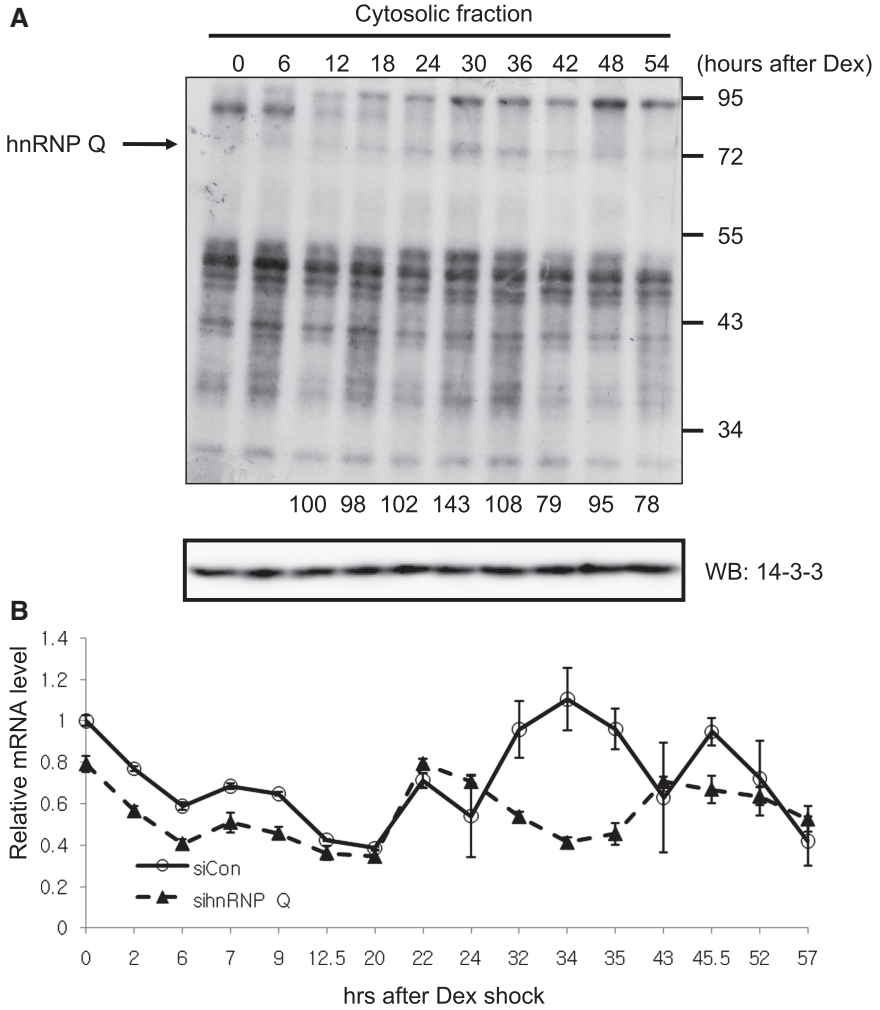

Figure 6. hnRNP Q interacts with m*Per3* 5′-UTR dynamically and is necessary for the robust oscillation m*Per3* mRNA. (**A**) Dynamics of the binding affinity of several proteins to m*Per3* 5′-UTR mRNA after synchronization was analyzed with the UV crosslinking assay (upper panel). The loading amounts of cytosolic extracts were confirmed by western blotting of the 14-3-3 level (lower panel). The normalized band intensities of hnRNP Q are shown below the upper panel. The intensity at 12 h after synchronization was arbitrarily set as 100. (**B**) The endogenous m*Per3* mRNA levels were determined using quantitative real-time RT–PCR and normalized to RPL32 mRNA levels at the indicated time points in phase-synchronized control siRNA or hnRNP Q siRNA-transfected NIH3T3 cells. Initial levels of m*Per3* mRNA in control siRNA-transfected cells were arbitrarily set as 1.0. These results represent the mean ± SD of three experiments.

between cytosolic hnRNP Q and 5′-UTR of m*Per3*. Overall, even though hnRNP Q did not bind to 5′-UTR of m*Per3* transcript in abundance, this interaction was highly enhanced 30–36 h after phase-synchronization with dexamethasone treatment (Figure 6A). Moreover, this time period was coincident with the declining phase that we already defined. To clarify the role of hnRNP Q in the oscillation of m*Per3* mRNA, we tranfected either a control siRNA or hnRNP Q siRNA into NIH3T3 fibroblasts, and synchronized a circadian phase of cells with dexamethasone treatment. Interestingly, we observed that overall oscillation phase of m*Per3* mRNA was advanced in hnRNP Q-downregulated cells. Moreover, the amplitude was evidently decreased in hnRNP Q-downregulated environment (Figure 6B) However, the oscillation pattern of mCry1 mRNA, another clock gene, was comparable in hnRNP Q-knockdowned condition (unpublished data). We also confirmed that oscillation phase of m*Per3* mRNA was unchanged when hnRNP R was downregulated (unpublished data). These results suggested that the precise regulation of the translation-mRNA decay coupling through hnRNP Q was necessary for the robust and scheduled oscillation of m*Per3*.

DISCUSSION

The regulation of mRNA decay rate, which is accomplished through changes in mRNA half-life, is an important step in the control of gene expression, as changes in mRNA abundance may alter the amount of the corresponding protein. For oscillating mRNAs, precise control of mRNA stability is even more critical because alterations to mRNA stability could affect the overall mRNA oscillation profile (16). A number of studies have shown that diverse stimuli have effects on the half-lives of mRNA (17,22–24). As for the circadian control of mRNA stability, the temporal regulation of

Drosophila period (*per*) mRNA stability was previously predicted by computer modeling based on the comparison of mRNA levels and transcription profiles (13). Given that circadian rhythm is a fundamental biological phenomenon (2), it is not surprising that the circadian rhythm regulates mRNA stability; however, little is known about the circadian regulation of mRNA stability.

In this study, we demonstrated that the turnover rate of m*Per3* mRNA was regulated by circadian rhythm, providing the first example of the circadian control of a clock gene whose mRNA stability is regulated by both of the 5′- and 3′-UTRs. This result implies that the molecular circadian rhythm could regulate the biological clock by controlling the mRNA stability of core clock genes. Given that the stability of TBP mRNA was independent of circadian rhythm (Figure 1B), the circadian regulation of the mRNA decay rate seems to be a specific phenomenon restricted to a subset of genes. In this regard, it will be interesting to identify the common features of those mRNAs whose stability is regulated according to circadian rhythm.

The UTRs of mRNA are known to play essential roles in post-transcriptional control, including the regulation of mRNA stability, subcellular localization, and translation efficiency (16,20,34,41). Many studies have focused on the independent functions of either the 5′-UTR or the 3′-UTR, nevertheless, the combined functions of the 5′- and 3′-UTRs were reported in some studies; the hypoxia-induced stabilization of *VEGF* mRNA was dependent on the cooperation of the 5′-UTR, 3′-UTR, and coding region (42); *Her-2* uORF-mediated translational inhibition was reversed by the *Her-2* 3′-UTR in cancer cells (43). Here, we showed that the circadian control of m*Per3* mRNA stability was also accomplished by the cooperative function of the 5′- and 3′-UTRs. The circadian regulation of mRNA stability was not mimicked by the 3′-UTR-mediated mRNA decay alone (Figure 2D) and required the additional function of the 5′-UTR.

As shown in Figure 4D, the cooperative function of the 5′- and 3′-UTRs reproduced the decay kinetics of endogenous m*Per3* mRNA in the rising phase. Nevertheless, since the Luc mRNA with both the 5′- and 3′-UTRs (i.e. 5′-UTR-Luc-3′-UTR) was a little more stable than the endogenous m*Per3* mRNA in the declining phase (Figures 1B and 4D), it should be noted that an additional region of m*Per3* mRNA seems to be needed to fully reproduce the decay kinetics observed in the declining phase. The missing region may be located in the coding region of m*Per3* mRNA, like *VEGF* mRNA (42) or *c-fos* mRNA (39).

Even though the 5′-UTR alone can mediate translational regulation-coupled mRNA decay (Figure 3B and C), circadian control of m*Per3* mRNA stability was not sufficiently regulated with only the 5′-UTR, given that the Luc mRNA with the m*Per3* 5′-UTR was degraded with almost the same rate in the rising and declining phases (unpublished data). Our results suggest that the functional role of the m*Per3* 3′-UTR in mRNA decay process is necessary in addition to the 5′-UTR.

We already verified that hnRNP Q could control the translation initiation of AANAT via an internal ribosomal entry site-mediated translation. However, we could not figure out any internal ribosomal entry site in 5′-UTR of m*Per3* (unpublished data) by using a dicistronic vector system (30). In this study, it is likely that hnRNP Q controls the translation of m*Per3* in a cap-dependent manner rather than in a cap-independent manner. Although knockdown of hnRNP Q resulted in inefficient mRNA decay of m*Per3*, overall m*Per3* mRNA level was less in sihnRNP Q-transfected cells than in siCon-transfected cells. This result remains a possibility that hnRNP Q is also involved in the transcriptional regulation of m*Per3*. Indeed, it has been reported that several hnRNP proteins participate in transcription regulation (44,45). In addition, it was recently identified that hnRNP Q has a critical role in splicing events (46). Indeed, there are four m*Per3* transcripts mediated by alternative splicing or alternative promoter, according to ASTD database (47). Therefore, it will be worthwhile to explore whether hnRNP Q can function as a transcriptional (co)factor or splicing factor on m*Per3*.

Our previous report demonstrated that the functional role of the m*Per3* 3′-UTR in the mRNA decay process contributed to the oscillation pattern of mRNA. In addition, the present study revealed that m*Per3* mRNA stability is also regulated in a circadian phase-dependent manner. It is the first evidence that the cooperative function of the 5′- and 3′-UTRs is necessary for the circadian control of the m*Per3* mRNA profile and decay rate. Results from the transfection of mRNA and the comparison of mRNA levels with Luc activity suggested that translational regulation-coupled mRNA decay is the underlying mechanism controlling m*Per3* mRNA stability. Although the mechanism of translation inhibition leading to the upregulation of mRNA stability still need to be determined, we suggest that translational regulation-coupled mRNA decay could be one of the possible mechanisms, which explains the distinct phase-lag between mRNA and protein levels.

SUPPLEMENTARY DATA

Supplementary Data are available at NAR Online.

ACKNOWLEDGEMENTS

The authors thank Ms Jiwon Lee for technical assistance. The authors also thank Dr Kiyoung Paek for experimental comments.

FUNDING

Funding for open access charge: Core Research Program/ Anti-aging and Well-being Research Center; the Brain Korea 21 program; World Class University program (R31-10105) of the Ministry of Education, Science and Technology; National Research Foundation of Korea (NRF; 20100002146, 20100019706 and 20100030089).

Conflict of interest statement. None declared.

REFERENCES

1. Reppert,S.M. and Weaver,D.R. (2002) Coordination of circadian timing in mammals. *Nature*, **418**, 935–941.
2. Bell-Pedersen,D., Cassone,V.M., Earnest,D.J., Golden,S.S., Hardin,P.E., Thomas,T.L. and Zoran,M.J. (2005) Circadian rhythms from multiple oscillators: lessons from diverse organisms. *Nat. Rev. Genet.*, **6**, 544–556.
3. Reppert,S.M. and Weaver,D.R. (2001) Molecular analysis of mammalian circadian rhythms. *Annu. Rev. Physiol.*, **63**, 647–676.
4. Ueda,H.R., Hayashi,S., Chen,W., Sano,M., Machida,M., Shigeyoshi,Y., Iino,M. and Hashimoto,S. (2005) System-level identification of transcriptional circuits underlying mammalian circadian clocks. *Nat. Genet.*, **37**, 187–192.
5. Hardin,P.E. (2004) Transcription regulation within the circadian clock: the E-box and beyond. *J. Biol. Rhythms*, **19**, 348–360.
6. Reppert,S.M. and Weaver,D.R. (2000) Comparing clockworks: mouse versus fly. *J. Biol. Rhythms*, **15**, 357–364.
7. Yamamoto,T., Nakahata,Y., Soma,H., Akashi,M., Mamine,T. and Takumi,T. (2004) Transcriptional oscillation of canonical clck genes in mouse peripheral tissues. *BMC Mol. Biol.*, **5**, 18.
8. Hardin,P.E., Hall,J.C. and Rosbash,M. (1992) Circadian oscillations in period gene mRNA levels are transcriptionally regulated. *Proc. Natl Acad. Sci. USA*, **89**, 11711–11715.
9. Darlington,T.K., Lyons,L.C., Hardin,P.E. and Kay,S.A. (2000) The period E-box is sufficient to drive circadian oscillation of transcription in vivo. *J. Biol. Rhythms*, **15**, 462–471.
10. Wang,G.K., Ousley,A., Darlington,T.K., Chen,D., Chen,Y., Fu,W., Hickman,L.J., Kay,S.A. and Sehgal,A. (2001) Regulation of the cycling of timeless (tim) RNA. *J. Neurobiol.*, **47**, 161–175.
11. Yoo,S.H., Ko,C.H., Lowrey,P.L., Buhr,E.D., Song,E.J., Chang,S., Yoo,O.J., Yamazaki,S., Lee,C. and Takahashi,J.S. (2005) A noncanonical E-box enhancer drives mouse Period2 circadian oscillations in vivo. *Proc. Natl Acad. Sci. USA*, **102**, 2608–2613.
12. Chen,Y., Hunter-Ensor,M., Schotland,P. and Sehgal,A. (1998) Alterations of per RNA in noncoding regions affect periodicity of circadian behavioral rhythms. *J. Biol. Rhythms*, **13**, 364–379.
13. So,W.V. and Rosbash,M. (1997) Post-transcriptional regulation contributes to Drosophila clock gene mRNA cycling. *EMBO J.*, **16**, 7146–7155.
14. Frisch,B., Hardin,P.E., Hamblen-Coyle,M.J., Rosbash,M. and Hall,J.C. (1994) A promoterless period gene mediates behavioral rhythmicity and cyclical per expression in a restricted subset of the Drosophila nervous system. *Neuron*, **12**, 555–570.
15. Stanewsky,R., Jamison,C.F., Plautz,J.D., Kay,S.A. and Hall,J.C. (1997) Multiple circadian-regulated elements contribute to cycling period gene expression in Drosophila. *EMBO J.*, **16**, 5006–5018.
16. Kwak,E., Kim,T.D. and Kim,K.T. (2006) Essential role of 3′-untranslated region-mediated mRNA decay in circadian oscillations of mouse Period3 mRNA. *J. Biol. Chem.*, **281**, 19100–19106.
17. Ross,J. (1995) mRNA stability in mammalian cells. *Microbiol. Rev.*, **59**, 423–450.
18. Wilusz,C.J., Wormington,M. and Peltz,S.W. (2001) The cap-to-tail guide to mRNA turnover. *Nat. Rev. Mol. Cell Biol.*, **2**, 237–246.
19. Tourriere,H., Chebli,K. and Tazi,J. (2002) mRNA degradation machines in eukaryotic cells. *Biochimie*, **84**, 821–837.
20. Guhaniyogi,J. and Brewer,G. (2001) Regulation of mRNA stability in mammalian cells. *Gene*, **265**, 11–23.
21. Woo,K.C., Kim,T.D., Lee,K.H., Kim,D.Y., Kim,W., Lee,K.Y. and Kim,K.T. (2009) Mouse period 2 mRNA circadian oscillation is modulated by PTB-mediated rhythmic mRNA degradation. *Nucleic Acids Res.*, **37**, 26–37.
22. Paulding,W.R. and Czyzyk-Krzeska,M.F. (2000) Hypoxia-induced regulation of mRNA stability. *Adv. Exp. Med. Biol.*, **475**, 111–121.
23. Staton,J.M., Thomson,A.M. and Leedman,P.J. (2000) Hormonal regulation of mRNA stability and RNA-protein interactions in the pituitary. *J. Mol. Endocrinol.*, **25**, 17–34.
24. Gorospe,M., Kumar,S. and Baglioni,C. (1993) Tumor necrosis factor increases stability of interleukin-1 mRNA by activating protein kinase C. *J. Biol. Chem.*, **268**, 6214–6220.
25. Lidder,P., Gutierrez,R.A., Salome,P.A., McClung,C.R. and Green,P.J. (2005) Circadian control of messenger RNA stability. Association with a sequence-specific messenger RNA decay pathway. *Plant Physiol.*, **138**, 2374–2385.
26. Yagita,K., Tamanini,F., van Der Horst,G.T. and Okamura,H. (2001) Molecular mechanisms of the biological clock in cultured fibroblasts. *Science*, **292**, 278–281.
27. Balsalobre,A., Damiola,F. and Schibler,U. (1998) A serum shock induces circadian gene expression in mammalian tissue culture cells. *Cell*, **93**, 929–937.
28. Ueda,H.R., Chen,W., Adachi,A., Wakamatsu,H., Hayashi,S., Takasugi,T., Nagano,M., Nakahama,K., Suzuki,Y., Sugano,S. *et al.* (2002) A transcription factor response element for gene expression during circadian night. *Nature*, **418**, 534–539.
29. Nagoshi,E., Saini,C., Bauer,C., Laroche,T., Naef,F. and Schibler,U. (2004) Circadian gene expression in individual fibroblasts: cell-autonomous and self-sustained oscillators pass time to daughter cells. *Cell*, **119**, 693–705.
30. Kim,T.D., Woo,K.C., Cho,S., Ha,D.C., Jang,S.K. and Kim,K.T. (2007) Rhythmic control of AANAT translation by hnRNP Q in circadian melatonin production. *Genes Dev.*, **21**, 797–810.
31. Ganguly,S., Coon,S.L. and Klein,D.C. (2002) Control of melatonin synthesis in the mammalian pineal gland: the critical role of serotonin acetylation. *Cell Tissue Res.*, **309**, 127–137.
32. Kim,T.D., Kim,J.S., Kim,J.H., Myung,J., Chae,H.D., Woo,K.C., Jang,S.K., Koh,D.S. and Kim,K.T. (2005) Rhythmic serotonin N-acetyltransferase mRNA degradation is essential for the maintenance of its circadian oscillation. *Mol. Cell Biol.*, **25**, 3232–3246.
33. Gray,N.K. and Wickens,M. (1998) Control of translation initiation in animals. *Annu. Rev. Cell Dev. Biol.*, **14**, 399–458.
34. Wilkie,G.S., Dickson,K.S. and Gray,N.K. (2003) Regulation of mRNA translation by 5′- and 3′-UTR-binding factors. *Trends Biochem. Sci.*, **28**, 182–188.
35. Savant-Bhonsale,S. and Cleveland,D.W. (1992) Evidence for instability of mRNAs containing AUUUA motifs mediated through translation-dependent assembly of a $>$20S degradation complex. *Genes Dev.*, **6**, 1927–1939.
36. Aharon,T. and Schneider,R.J. (1993) Selective destabilization of short-lived mRNAs with the granulocyte-macrophage colony-stimulating factor AU-rich 3′ noncoding region is mediated by a cotranslational mechanism. *Mol. Cell Biol.*, **13**, 1971–1980.
37. Winstall,E., Gamache,M. and Raymond,V. (1995) Rapid mRNA degradation mediated by the c-fos 3′ AU-rich element and that mediated by the granulocyte-macrophage colony-stimulating factor 3′ AU-rich element occur through similar polysome-associated mechanisms. *Mol. Cell Biol.*, **15**, 3796–3804.
38. Curatola,A.M., Nadal,M.S. and Schneider,R.J. (1995) Rapid degradation of AU-rich element (ARE) mRNAs is activated by ribosome transit and blocked by secondary structure at any position 5′ to the ARE. *Mol. Cell Biol.*, **15**, 6331–6340.
39. Schiavi,S.C., Wellington,C.L., Shyu,A.B., Chen,C.Y., Greenberg,M.E. and Belasco,J.G. (1994) Multiple elements in the c-fos protein-coding region facilitate mRNA deadenylation and decay by a mechanism coupled to translation. *J. Biol. Chem.*, **269**, 3441–3448.
40. Kim,D.Y., Woo,K.C., Lee,K.H., Kim,T.D. and Kim,K.T. (2010) hnRNP Q and PTB modulate the circadian oscillation of mouse Rev-erb alpha via IRES-mediated translation. *Nucleic Acids Res.*, **38**, 7068–7078.
41. Mignone,F., Gissi,C., Liuni,S. and Pesole,G. (2002) Untranslated regions of mRNAs. *Genome Biol.*, **3**, REVIEWS0004.
42. Dibbens,J.A., Miller,D.L., Damert,A., Risau,W., Vadas,M.A. and Goodall,G.J. (1999) Hypoxic regulation of vascular endothelial growth factor mRNA stability requires the cooperation of multiple RNA elements. *Mol. Biol. Cell.*, **10**, 907–919.
43. Mehta,A., Trotta,C.R. and Peltz,S.W. (2006) Derepression of the Her-2 uORF is mediated by a novel post-transcriptional control mechanism in cancer cells. *Genes Dev.*, **20**, 939–953.

44. Rauch,J., O'Neill,E., Mack,B., Matthias,C., Munz,M., Kolch,W. and Gires,O. (2010) Heterogeneous nuclear ribonucleoprotein H blocks MST2-mediated apoptosis in cancer cells by regulating A-Raf transcription. *Cancer Res.*, **70**, 1679–1688.
45. Li,H. and Liu,J. (2010) Identification of heterogeneous nuclear ribonucleoprotein K as a transactivator for human low density lipoprotein receptor gene transcription. *J. Biol. Chem.*, **285**, 17789–17797.
46. Chen,H.H., Chang,J.G., Lu,R.M., Peng,T.Y. and Tarn,W.Y. (2008) The RNA binding protein hnRNP Q modulates the utilization of exon 7 in the survival motor neuron 2 (SMN2) gene. *Mol. Cell Biol.*, **28**, 6929–6938.
47. Koscielny,G., Le Texier,V., Gopalakrishnan,C., Kumanduri,V., Riethoven,J.J., Nardone,F., Stanley,E., Fallsehr,C., Hofmann,O., Kull,M. *et al.* (2009) ASTD: The Alternative Splicing and Transcript Diversity database. *Genomics*, **93**, 213–220.